Quantitative assessment of prefrontal cortex in humans relative to nonhuman primates

Chad J. Donahue[a,1], Matthew F. Glasser[a,b], Todd M. Preuss[c,d,e], James K. Rilling[d,e,f,g,h], and David C. Van Essen[a,1]

[a]Department of Neuroscience, Washington University School of Medicine, St. Louis, MO 63110; [b]St. Luke's Hospital, St. Louis, MO 63017; [c]Division of Neuropharmacology and Neurologic Diseases, Emory University, Atlanta, GA 30329; [d]Center for Translational Social Neuroscience, Emory University, Atlanta, GA 30329; [e]Yerkes National Primate Research Center, Emory University, Atlanta, GA 30329; [f]Department of Anthropology, Emory University, Atlanta, GA 30329; [g]Center for Behavioral Neuroscience, Emory University, Atlanta, GA 30329; and [h]Department of Psychiatry and Behavioral Sciences, Emory University, Atlanta, GA 30329

Contributed by David C. Van Essen, March 22, 2018 (sent for review December 14, 2017; reviewed by Leah A. Krubitzer, Rogier Mars, and Jeroen B. Smaers)

Humans have the largest cerebral cortex among primates. The question of whether association cortex, particularly prefrontal cortex (PFC), is disproportionately larger in humans compared with nonhuman primates is controversial: Some studies report that human PFC is relatively larger, whereas others report a more uniform PFC scaling. We address this controversy using MRI-derived cortical surfaces of many individual humans, chimpanzees, and macaques. We present two parcellation-based PFC delineations based on cytoarchitecture and function and show that a previously used morphological surrogate (cortex anterior to the genu of the corpus callosum) substantially underestimates PFC extent, especially in humans. We find that the proportion of cortical gray matter occupied by PFC in humans is up to 1.9-fold greater than in macaques and 1.2-fold greater than in chimpanzees. The disparity is even more prominent for the proportion of subcortical white matter underlying the PFC, which is 2.4-fold greater in humans than in macaques and 1.7-fold greater than in chimpanzees.

neuroanatomy | prefrontal cortex | evolution | cortical parcellation | chimpanzee

Cerebral cortex varies dramatically in size and surface area across mammals. Human cortex is the largest among primates, with a surface area roughly threefold larger than in chimpanzees and about 10-fold larger than in the intensively studied macaque monkey (1–6). Many studies have reported that association cortex [prefrontal, temporal, and parietal regions implicated in higher cognition and affect (7–9)] is disproportionately larger in humans relative to nonhuman primates (10–16). However, other studies report different conclusions, especially for prefrontal cortex (PFC) (17–19), resulting in an ongoing controversy (20).

Analyses of this type are often viewed through the lens of allometry by comparing the size of a given brain region with another measure, such as overall brain size, across a range of species. Allometric scaling implies a linear relationship when plotting data on a logarithmically scaled plot, where the slope of the best-fitting line may show positive (slope >1; hypermetric), isometric (slope = 1), or negative (slope <1; hypometric) allometry. Furthermore, a significant positive deviation of a single species from an allometric relationship would be referred to as "exceptional" [e.g., human brain weight relative to body weight is exceptionally large compared with other mammals (21)]. Some studies have reported a positive allometric relationship across primate species based on the size of the PFC and the rest of the brain using structural volumes (18, 22). Others have compared PFC to lower-order cortical areas and reported a deviation in humans from the allometric trend when comparing the size of the PFC with that of primary visual (area V1) and frontal motor cortex (12, 23). In contrast, Gabi et al. (17) recently reported evidence for an isometric relationship using neuronal counts for PFC vs. other cortical regions.

Other morphometric analyses inform but do not resolve this debate. Semendeferi et al. (19, 24) reported that although frontal, temporal, and parietal lobes are larger in humans than in apes, the fraction of total cortex belonging to each region is similar across species. By contrast, studies using surface-based interspecies registration (mapping) constrained by putative cortical homologs suggest that surface area in these regions is disproportionately larger (20-fold or more in places) in humans compared with macaques, whereas early sensory regions (e.g., area V1) are expanded as little as twofold (3–5); there are also regional differences in estimated PFC extent when comparing marmoset, capuchin, and macaque monkeys (25). Furthermore, cortical myelin maps derived from in vivo MRI reveal a greater extent of lightly myelinated cortex in both association and higher-order sensory regions in humans compared with chimpanzees and macaques, whereas species differences appear more modest in heavily myelinated early sensorimotor regions (6).

These conflicting results and interpretations regarding PFC scaling may largely reflect methodological differences among studies (20, 23). One such difference is the region with which the PFC is being compared. Bush and Allman (22) compared frontal

Significance

A longstanding controversy in neuroscience pertains to differences in human prefrontal cortex (PFC) compared with other primate species; specifically, is human PFC disproportionately large? Distinctively human behavioral capacities related to higher cognition and affect presumably arose from evolutionary modifications since humans and great apes diverged from a common ancestor about 6–8 Mya. Accurate determination of regional differences in the amount of cortical gray and subcortical white matter content in humans, great apes, and Old World monkeys can further our understanding of the link between structure and function of the human brain. Using tissue volume analyses, we show a disproportionately large amount of gray and white matter corresponding to PFC in humans compared with nonhuman primates.

Author contributions: C.J.D., M.F.G., and D.C.V.E. designed research; C.J.D. performed research; C.J.D., M.F.G., T.M.P., J.K.R., and D.C.V.E. analyzed data; and C.J.D., M.F.G., T.M.P., J.K.R., and D.C.V.E. wrote the paper.

Reviewers: L.A.K., University of California, Davis; R.M., Radboud University Nijmegen; and J.B.S., Stony Brook University.

The authors declare no conflict of interest.

Data deposition: All data related to this study are freely available via the BALSA database (https://balsa.wustl.edu/study/zlVX).

[1]To whom correspondence may be addressed. Email: donahuec@wustl.edu or vanessen@wustl.edu.

This article contains supporting information online at www.pnas.org/lookup/suppl/doi:10.1073/pnas.1721653115/-/DCSupplemental.

Published online May 8, 2018.

gray matter with remaining neocortical gray matter, whereas Smaers et al. (23) compared the PFC with more evolutionarily conserved, lower-order cortical regions such as primary visual cortex (area V1). Some studies focus on volumetric differences in cortical gray matter and/or the extent of the underlying white matter (26), whereas others consider counts of neurons for gray matter and nonneuronal cells for white matter (17). Most striking are differences in delineating what constitutes the PFC. A lack of comparative architectonic or other data that could directly identify the location of homologous areas and regions has led some investigators to instead invoke neuroanatomical proxies for the PFC. For example, Semendeferi et al. (19) analyzed the entire frontal lobe, whereas Smaers et al. (27) investigated cumulative frontal lobe volumes starting respectively from its anterior (prefrontal) and posterior (motor) extremes. Schoenemann et al. (26) and Gabi et al. (17) explicitly approximated the PFC using a morphological surrogate: cortex anterior to the genu of the corpus callosum. However, the accuracy of this genu-based approximation has yet to be critically assessed.

Generally, "PFC" has referred to frontal lobe association cortex lying anterior to motor and premotor regions. Many studies have used cytoarchitectonics in efforts to objectively delineate the PFC. Cortical layer 4 can appear granular (with a high density of small neurons), agranular (lacking a well-defined layer 4), or dysgranular (having a subtle layer 4 with a modest density of small neurons). The earliest delineation of the PFC was Brodmann's (15) *regio frontalis*, consisting of granular frontal and orbital cortex. More recent studies consider the PFC to include both granular and dysgranular regions of medial frontal and orbitofrontal cortex in human (28) and macaque (29) and lateral frontal cortex in both species (30–32). Geyer (33) analyzed human premotor and prefrontal regions and reported that agranular cortex in posterior Brodmann area 6 (premotor) transitions anteriorly to dysgranular cortex by a graded cytoarchitectonic transition rather than by a sharp boundary. Consistent with this hypothesis, functional neuroimaging analyses implicate some agranular as well as dysgranular frontal lobe areas in higher cognitive function (34).

To address differences in PFC across several primate species, we used structural MRI datasets from humans, chimpanzees, and macaque monkeys to generate cortical surface models of individual subjects, estimate cortical myelin content and thickness, and register individuals to species-average atlases. We then utilized available data to delineate the PFC in several ways. We present PFC delineations based on architectonic criteria and on the callosal genu PFC approximation in all three species and on combined functional and architectonic criteria for humans and macaques. Because we analyzed only three species, we could not create a robust nonhuman primate allometric scaling regression to evaluate whether data points for humans are exceptional. Instead, we focus on the relative scaling of the PFC across species compared with non-PFC cortex, area V1, and area 4.

Results

Cytoarchitectural Designations Allow Surface-Based PFC Delineation Across Species. Based on cytoarchitectonics, we delineated a conservative PFC boundary (Fig. 1, regions filled in red) that includes granular and dysgranular frontal lobe cortex anterior to motor and premotor cortex, as has been proposed for both humans (28, 31) and macaques (35). However, agranular regions of medial frontal and orbitofrontal cortex have been implicated in higher cognitive function, and we consider it appropriate to include these areas of frontal lobe cortex that are functionally neither motor nor premotor in a liberal PFC delineation (Fig. 1, additional regions filled in blue).

For human cortex, we used individual-subject parcellations from 60 unrelated subjects taken from the 210V group [the validation group of the Human Connectome Project (HCP) Multimodal Parcellation (HCP_MMP1.0), which used an areal classifier that matched individual-subject feature vectors to an initial group-average multimodal parcellation (34)]. For the

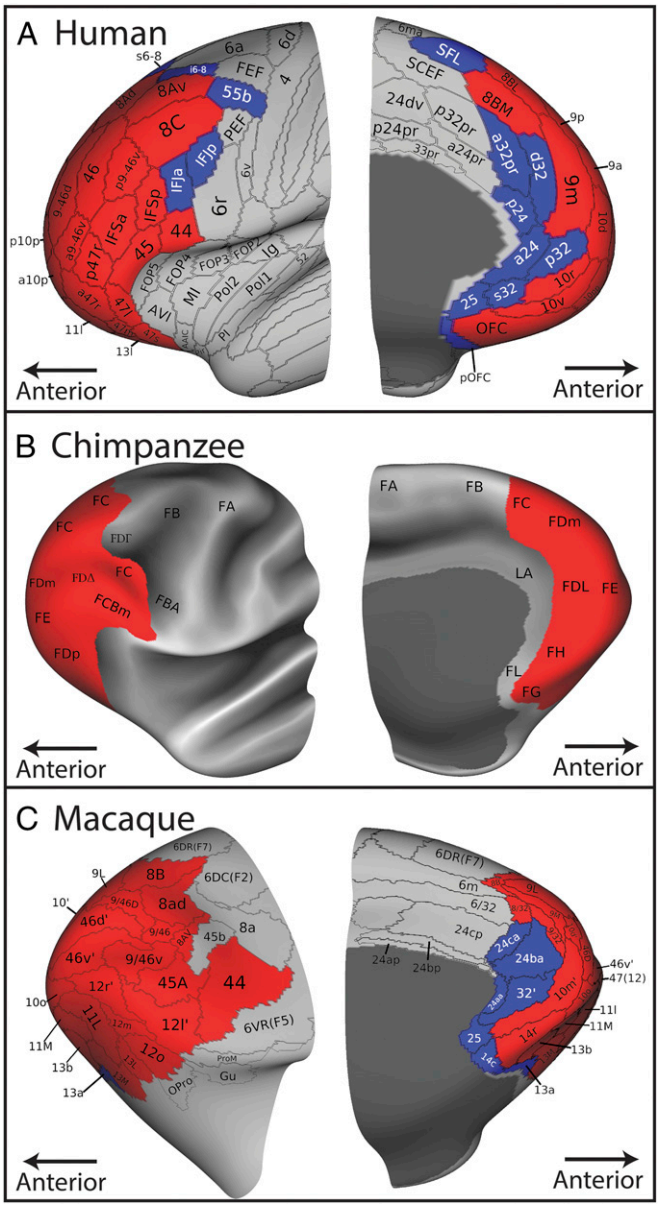

Fig. 1. Parcellations of prefrontal cortex for human, macaque, and chimpanzee displayed on inflated (unfolded) left hemisphere surfaces cropped to include only anterior regions for lateral (*Left*) and medial (*Right*) views of each species. (*A*) Inflated human cortical surface displaying group-average HCP_MMP1.0 parcellation. Conservative PFC includes red areas. Liberal PFC additionally includes blue areas. (*B*) Inflated chimpanzee cortical surface displaying a conservative PFC delineation based on the Bailey et al. (42) cytoarchitectonic parcellation and maps/gradients of cortical myelin content. (*C*) Inflated macaque cortical surface displaying a composite parcellation adapted from three studies (36–38) along with conservative and liberal PFC delineations. Figures are not to scale. Data are available at https://balsa.wustl.edu/GrK7 (human), https://balsa.wustl.edu/px4G (chimpanzee), and https://balsa.wustl.edu/k94P (macaque).

macaque, a pan-hemispheric composite of published parcellations (36–38) was mapped onto a species-average macaque atlas (39) (Yerkes19) and then to the constituent 19 individuals for morphometric analyses. This composite includes several modified areas, marked as "prime," that reflect a combination of previously described areas. For example, area 10′ found in dorsolateral PFC is an amalgamation of area 10 as reported by Ferry et al. (36) and Paxinos et al. (38). Some of these areas then

underwent further subdivision: areas 24a, 24b, and 24c were subdivided into anterior and posterior segments (e.g., 24aa and 24ap, respectively) based on descriptions of area 24 as dysgranular anteriorly with associated cognitive-related function transitioning to an agranular cytoarchitecture posteriorly associated with motor function (30, 40, 41). The Bailey et al. chimpanzee architectonic parcellation (42) includes areal designations on a series of histological section contours. We mapped areal designations from section contours to corresponding MRI sections in an individual chimpanzee brain and from there to our surface-based chimpanzee atlas (*Supporting Information*). We then drew estimated areal boundaries on the atlas surface, aided in dorsolateral cortex by myelin maps, cortical thickness maps, and their gradients.

For each species, an area was considered part of conservative PFC based on cytoarchitecture and inclusion in published PFC delineations. Areas specific to the human liberal PFC delineation include inferior frontal junction areas (IFJa/p), i/s6-8, and 55b of the lateral frontal cortex, a/p24, 25, a32pr, d/p/s32, and the superior frontal language area (SFL) of the medial frontal cortex, and posterior orbitofrontal cortex (pOFC). For the macaque, exclusively liberal PFC areas include medial frontal areas 24aa, 24ba, 24ca, 25, and 32′ and orbitofrontal areas 13a and 14c. The frontal eye fields are sometimes considered part of the PFC (40, 43) but were excluded here because of their stronger association with premotor regions than with cognitive regions in terms of moderate rather than sparse myelin content and their functional connectivity (34). Frontal eye fields correspond to the frontal eye field (FEF) and premotor eye field (PEF) areas in humans; area 45b in the macaque is moderately myelinated and overlaps with anatomically and functionally defined FEF (44). Given the paucity of functional data for the chimpanzee, we focused only on a conservative PFC delineation based on the presence of granular/dysgranular cytoarchitecture and on myelin patterns. We identified Bailey et al. agranular areas as motor (FA), premotor (FB and FBA), and cingulate (LA and FL). More anterior regions were designated as PFC, except for FDΓ, which is moderately myelinated and likely corresponds to FEF. Medially, our chimpanzee PFC delineation includes areas FDL, FH, and FG but excludes LA and FL. (See *Supporting Information* for additional details and discussion of putative homologs. Figure S1 illustrates the chimpanzee parcellation. Tables S2 and S3 provide information and references for areal cytoarchitecture and cognitive-related designations for human and macaque PFC areas.)

Structural Cortical Features Aid in Delineating the PFC. Maps of estimated myelin content based on the T1-weighted/T2-weighted (T1w/T2w) intensity ratio (6, 45) provide a useful architectural marker for identifying cortical regions and areas across species. Spatial gradients of these myelin maps can provide objective evidence of sharply defined architectonic transitions (e.g., from dense to moderate or light myelination; see ref. 45). Fig. 2 illustrates myelin maps and their spatial gradients for each species in relation to our three PFC delineations. These reveal important patterns and correlations across measures, but the relationship to PFC boundaries is complex and differs for dorsolateral, ventrolateral, and medial regions.

In dorsolateral cortex, the heavily myelinated primary motor cortex (area 4; Fig. 2, *Top Row*, outlined in black) and the moderately myelinated premotor strip (directly anterior to area

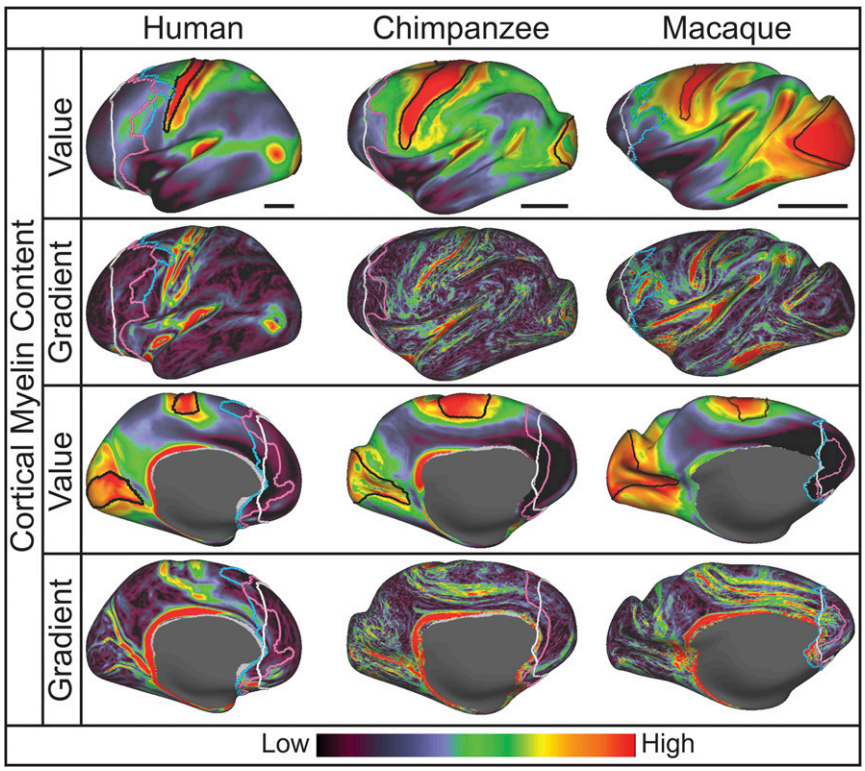

Fig. 2. Structural features of lateral (*Top* and *Second Rows*) and medial (*Third* and *Bottom Rows*) inflated left hemisphere cortex related to delineations of the PFC. Each primate species cortical surface displays myelin content (*Top* and *Third Rows*) and its corresponding spatial gradient (*Second* and *Bottom Rows*). The white line overlying each map represents the group-average location of the coronal slice at the corpus callosum genu (see also Fig. 3); pink and blue lines represent group-average conservative and liberal PFC delineations, respectively. Primary motor area 4 and primary visual area V1 are bounded by black contours in the parietal and occipital cortex, respectively. Black bars indicate the relative scale of the group-average inflated surfaces for each species. Data are available at https://balsa.wustl.edu/22XL.

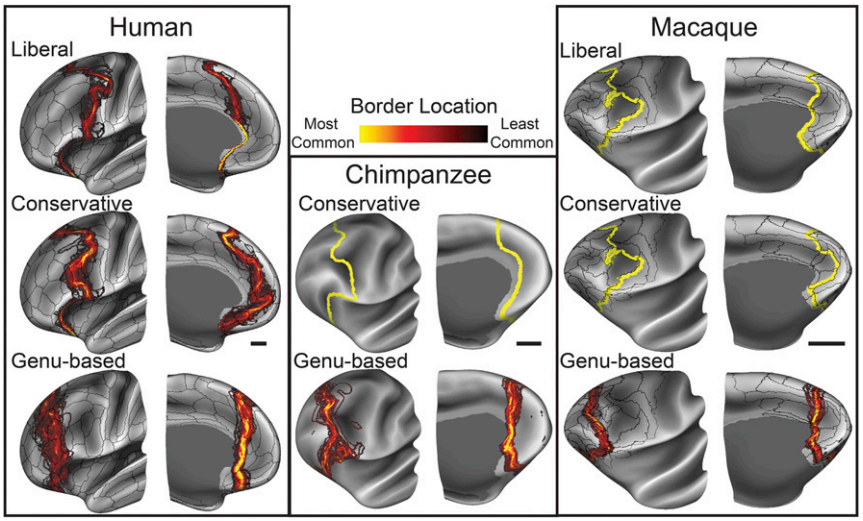

Fig. 3. PFC border probability maps displayed on inflated left hemisphere atlas surfaces of the frontal lobe (*Left*, lateral aspect; *Right*, medial aspect of each pair) overlaid on group-average sulcal depth maps. Human liberal and conservative PFC borders were created using individual subject parcellations, resulting in pronounced intersubject variance on the group-average surface. Corresponding borders in the macaque and chimpanzee were created using a group-average parcellation registered to each individual subject and thus show no such variance. Black bars indicate the relative scale for the group-average inflated surfaces. Data are available at https://balsa.wustl.edu/r7Xw (human), https://balsa.wustl.edu/xMp4 (chimpanzee), and https://balsa.wustl.edu/PMKk (macaque).

4; mainly green in human; green and yellow in chimpanzee, mainly orange-yellow in macaque) provide useful landmarks across species. In the macaque, the thickness map and its gradient were also useful, particularly for posterior area 4 (*Supporting Information*). In all three species, a myelin gradient ridge (Fig. 2, *Second Row*) runs along part of the anterior border of area 4. Anterior to this premotor/primary motor gradient ridge is another gradient ridge. In the human, this anterior gradient ridge aligns well with the liberal PFC border. In the macaque, both conservative and liberal PFC borders run in the general vicinity of the anterior myelin gradient ridges, but the correlation is not good for either. The border of chimpanzee conservative PFC follows the ridge closely in this region.

In ventrolateral and ventral regions, lightly myelinated PFC in all three species is adjoined by even more lightly myelinated cortex in the anterior insula (Fig. 2, *Top Row*, indigo and black) and orbitofrontal cortex (Fig. 2, *Third Row*). However, the most prominent myelin gradient does not coincide with published architectonic PFC delineations [also, in the macaque and chimpanzee datasets, orbitofrontal cortex was not as accurately segmented owing to localized signal dropout and distortion of T1w relative to T2w images]. In medial cortex, the PFC is lightly myelinated dorsally and very lightly myelinated ventrally in all three species, but none of them shows a clear myelin gradient running along the PFC boundary. Thus, there are strong cross-species similarities in myelin maps in and near the PFC, but only in the dorsolateral PFC of human and chimpanzee do we consider myelin gradients strongly informative about PFC borders. Cortical thickness maps and their gradients were of limited utility for delineating PFC borders (Fig. S4).

Genu-Based Morphological Surrogate Underestimates PFC Extent. Fig. 3 illustrates the range of individual variation in the location of liberal, conservative, and genu-based PFC borders as defined for each species. Probability maps indicate most (yellow) and least (black) common locations of each border.

Important species differences are revealed by comparing parcellation-based PFC delineations (both liberal and conservative) with genu-based PFC approximations (Fig. 3, *Bottom Row*). In dorsolateral frontal cortex, the macaque and chimpanzee genu-based PFC border runs somewhat anterior to the moderately myelinated region adjacent to premotor cortex, mostly anterior to the conservative delineation. By visual inspection, the genu-based delineation in the human more substantially underestimates PFC spatial extent compared with both liberal and conservative delineations. This observation is evaluated quantitatively in the next section.

Human PFC Is Absolutely and Relatively Large Compared with Nonhuman Primates. Table 1 reports the mean volume for total cortical gray matter, primary visual area V1, and primary motor area 4 and mean volumes relating to PFC delineations, along with SDs. These volumes were calculated for both hemispheres of each individual subject and then were averaged. Also provided

Table 1. Cortical gray matter volumes across species

	Gray matter, cm^3					
Species	Total volume	Genu-based PFC (%)	Conservative PFC (%)	Liberal PFC (%)	Area V1 (%)	Area 4 (%)
Human (n = 60)	512 ± 55	77.2 ± 11 (15)	105 ± 13 (21)	131 ± 16 (26)	14.0 ± 2.0 (2.72)	11.2 ± 1.6 (2.18)
Chimpanzee (n = 29)	134 ± 13	18.5 ± 2.6 (14)	23.2 ± 2.4 (17)		7.5 ± 0.8 (5.63)	8.1 ± 1.2 (6.04)
Macaque (n = 19)	34.4 ± 2.9	3.34 ± 0.5 (10)	4.4 ± 0.5 (13)	4.8 ± 0.6 (14)	3.3 ± 0.4 (10.7)	1.4 ± 0.2 (4.46)

Mean volumes of human, chimpanzee, and macaque cortical gray matter for entire cortex; genu-based, conservative, and liberal delineations of prefrontal cortex; primary visual area V1, and primary motor area 4, as well as SDs. Percentages in parentheses are percentages of total cortical gray matter volume. See Dataset S1 for additional measures.

(in parentheses) is the percentage of each PFC region of interest (ROI) and cortical area volume relative to total volume of the neocortex (see *Supporting Information* for individual variance in percentage values and Dataset S1 for additional measures).

After averaging the left and right hemispheres, computed mean gray matter volumes were 512 ± 55 cm^3, 134 ± 13 cm^3, and 34.4 ± 2.9 cm^3 for human, chimpanzee, and macaque, respectively, indicating that the volume of human cortical gray matter is 15-fold greater than that in the macaque and roughly fourfold greater than that in the chimpanzee. Mean surface areas were 1,843 ± 196 cm^2 for humans, 599 ± 53 cm^2 for chimpanzees, and 193 ± 13 cm^2 for macaques; mean cortical thicknesses were 2.7 ± 0.1 mm, 2.6 ± 0.1 mm, and 2.0 ± 0.1 mm, respectively (SDs are of means across subjects).

As shown by our two parcellation-based delineations, the proportion of PFC gray matter volume is up to 1.9-fold greater in humans compared with macaques (26% vs. 14% for the liberal delineation; 21% vs. 13% for the conservative delineation) and 1.2-fold greater compared with chimpanzees (21% vs. 17% for the conservative delineation). The genu-based PFC approximation shows a more moderate species difference, constituting 15% of human cortical gray matter volume compared with 14% in the chimpanzee and 10% in the macaque. Cortical volume computed using the genu-based proxy for PFC underestimates the parcellation-based delineations in all three species but most prominently in humans.

Scaling Relative to Primary Visual and Motor Areas. To quantify how the PFC has scaled relative to more evolutionarily conserved cortical areas, we analyzed primary visual cortex (area V1) and primary motor cortex (area 4) in terms of their cortical gray matter volume, surface area, and cortical thickness in humans, chimpanzees, and macaques (see Fig. 2 for delineations, Dataset S1 for detailed measures, and *Supporting Information* for additional methodological details).

In humans, chimpanzees, and macaques, respectively, the mean V1 volume was 14.0 ± 2 cm^3, 7.5 ± 0.8 cm^3, and 3.3 ± 0.4 cm^3; the surface area was 69.7 ± 9.4 cm^2, 47.2 ± 4.7 cm^2, and 21.6 ± 1.8 cm^2; and the cortical thickness was 2.0 ± 0.1 mm, 2.0 ± 0.2 mm, and 1.8 ± 0.1 mm. The PFC volume is similar to that of V1 in the macaque but is severalfold larger than V1 in the chimpanzee and is up to ninefold larger than V1 in humans. Surface area followed a similar trend: PFC surface area is similar to that of V1 in the macaque but is up to 1.8-fold greater than V1 in chimpanzees and is sixfold greater in humans.

For primary motor area 4 in humans, chimpanzees, and macaques, respectively, the mean volume was 11.2 ± 1.6 cm^3, 8.1 ± 1.2 cm^3, and 1.4 ± 0.2 cm^3; the surface area was 39.4 ± 5.4 cm^2, 25.6 ± 3.1 cm^2, and 5.3 ± 0.5 cm^2; and the cortical thickness was 2.8 ± 0.1 mm, 2.6 ± 0.2 mm, and 2.9 ± 0.1 mm. Comparisons with PFC gray matter volumes in humans and chimpanzees shows a trend similar to that for area V1, as the PFC is roughly 12-fold larger than area 4 in humans and is threefold greater than area 4 in chimpanzees. However, macaque area 4 is only 42% of the V1 volume, and its PFC volume is threefold greater than that of area 4.

Table 2. Subcortical white matter volumes across species

Species	White matter, cm^3	
	Total volume	Genu-based PFC (%)
Human (n = 60)	443 ± 62	52.3 ± 10.2 (12)
Chimpanzee (n = 29)	119 ± 12	8.5 ± 1.9 (7)
Macaque (n = 19)	21.8 ± 2.5	1.1 ± 0.2 (5)

Volumes of human, chimpanzee, and macaque subcortical white matter for entire cortex and genu-based delineations of PFC. PFC percentages in parentheses are relative to total volume. See Dataset S1 for additional measures.

White Matter Volumes. Table 2 reports the total volume of subcortical white matter for each species along with volumes of white matter anterior to the genu-based PFC proxy, which is the only parcellation having a well-defined posterior extent of PFC white matter and hence amenable to analysis of white matter volumes. Total white matter volumes for humans, chimpanzees, and macaques were on average 443 ± 62 cm^3, 119 ± 12 cm^3, and 21.8 ± 2.5 cm^3, respectively (see Dataset S1 for additional measures).

The ratio of total white matter to gray matter volume is similar in the human and chimpanzee (0.87 and 0.89, respectively), considerably greater than that for the macaque (0.63), indicating a 35–40% relative increase in the total white matter-to-gray matter ratio in humans and chimpanzees relative to the macaque. Genu-based PFC white matter-to-gray matter ratios are 0.68 in human, 0.46 in chimpanzee, and 0.33 in macaque. Analyzed differently, PFC white matter is a larger fraction of total white matter in humans (12%) than in chimpanzees (7%) or macaques (5%). This 2.4-fold relative difference in PFC white

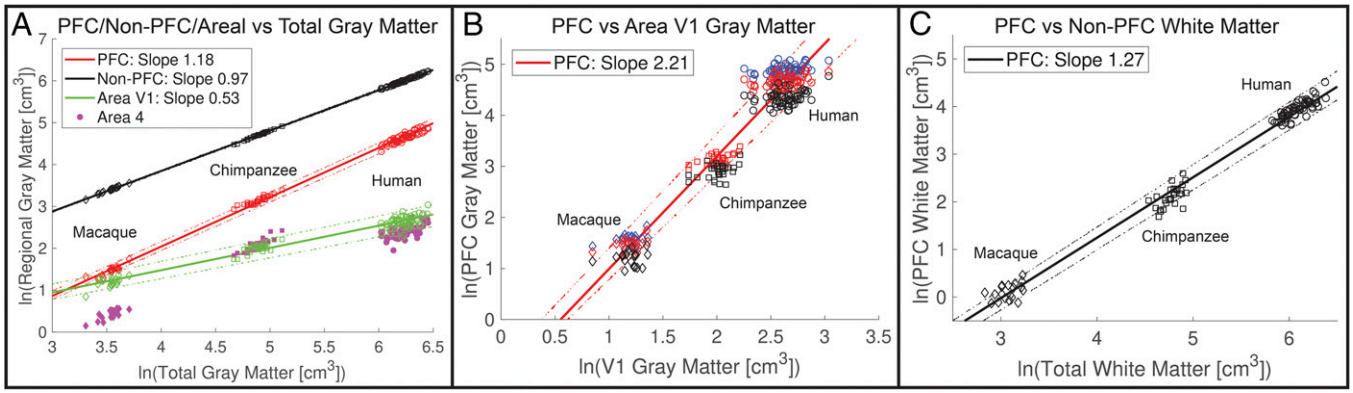

Fig. 4. Log-scale plots comparing PFC gray and white matter volume with reference values across species (macaques, diamonds; chimpanzees, squares; humans, circles). (*A*) Volumes of conservative PFC (red), non-PFC (black), and area V1 (green) gray matter plotted against total cortical gray matter volume. Volumes of area 4 are plotted with solid magenta markers without a corresponding linear fit. (*B*) PFC gray matter volume plotted against the volume of the primary visual cortex. Blue, red, and black markers indicate liberal, conservative, and genu-based PFC delineations, respectively. (*C*) Genu-based PFC white matter volume plotted against total white matter volume. For all panels, solid lines represent the best fit using mean macaque, chimpanzee, and human data points; dotted lines represent 95% CIs.

matter between humans and macaques (12% vs. 5%) markedly exceeds the 1.5-fold difference in the genu-based gray matter volumes.

PFC Exhibits Positive Allometric Scaling for Humans and Nonhuman Primates. Fig. 4 illustrates several logarithmically scaled comparisons that represent the size of the PFC across species relative to reference measures. To assess the differential scaling of different cortical regions, we plotted the volumes of PFC gray matter, non-PFC gray matter, area V1, and area 4 against the volume of total cortical gray matter (Fig. 4*A*). We additionally compared PFC gray matter with the more evolutionarily conserved area V1 (Fig. 4*B*) and compared PFC white matter with total white matter (Fig. 4*C*).

When using total cortical gray matter as a reference (Fig. 4*A*), the scaling of conservative PFC gray matter as defined by the regression line through the mean macaque, chimpanzee, and human data points exhibits positive allometry (slope of 1.18; 95% CI 1.16–1.18). Additionally, this regression of PFC across total cortex appears steeper than that of other comparators: non-PFC cortex (slope of 0.97; 95% CI 0.96–0.97) and visual area V1 (slope of 0.53; 95% CI 0.49–0.54). Analysis of covariance (ANCOVA) across the three regression slopes indicated they are significantly different from one another (*Supporting Information*). Interestingly, data for area 4 across the three species deviate markedly from an allometric fit (linear on a log–log plot). Area 4 volume is similar to that of V1 in humans and chimpanzees but is much smaller than that in the macaque (*Discussion*). When, instead, the evolutionarily conserved visual area V1 is used as a reference (Fig. 4*B*), the PFC scales with even greater positive allometry (slope of 2.21; 95% CI 2.05–2.24). Finally, PFC white matter scaled with total white matter volume with positive allometry (slope of 1.27; 95% CI 1.26–1.31).

Discussion

Using a cortical surface-based approach, we have presented a comparative delineation and analysis of frontal association cortex in humans, chimpanzees, and macaques. In addressing a longstanding controversy, we report strong evidence for a greater proportion of human PFC gray matter volume compared with two nonhuman primates and an even greater species difference for PFC white matter volume.

Prefrontal Cortex Can Be Delineated Using Cytoarchitectonic and Functional Criteria. Our criteria for areal inclusion in the PFC entailed judgment calls based on the preponderance of available evidence. Our conservative criteria relating to granular/dysgranular cytoarchitecture, although guided by evidence in the literature, is not a simple consensus view. Our liberal delineations in the human and macaque (areas reported to have agranular cytoarchitecture) entailed subjective assessments regarding what cognitive task contrast activation or other functional information relative to neighbors warrants inclusion. A notable exception to these criteria across species is the exclusion of frontal eye fields: area FEF in humans, 45b in macaques, and FDΓ in chimpanzees. While these areas are cytoarchitecturally granular/dysgranular and receive thalamic inputs primarily from the mediodorsal (MD) nucleus, their functional relationship to eye movement led to our placing them in the premotor category as opposed to cognitive-related PFC [see *Supporting Information* and *Supplementary neuroanatomical results* in Glasser et al. (34)]. Additionally, some areas in the macaque composite parcellation (e.g., anterior and posterior subdivisions of areas 24a, 24b, and 24c) might reasonably be reassigned to account for a gradient in cytoarchitecture, primarily in areas that extend posteriorly into densely myelinated cortex. However, plausible alternative choices for PFC extent in any of the species would not negate our main conclusion that the relative size of the PFC in the human lineage is larger than that in nonhuman primates. For example, inclusion of frontal eye field areas FEF and 45b in humans and macaques (0.52% of cortical gray matter volume in humans and 0.47% in the macaque; Dataset S1) would not materially affect our conclusions. For chimpanzees, the lack of functional imaging data limited our analysis to conservative and genu-based PFC delineations, which were guided by the Bailey et al. (42) cytoarchitectural atlas in terms of cytoarchitecture and plausibility of putative cortical homologs. These putative homologies were based on descriptions of cytoarchitecture and are by no means conclusive; however, they allowed a first-order comparison with humans and macaques. Explicit regional boundaries, however, were drawn based on visual inspection and comparison of maps of cortical myelin content, cortical thickness, and their associated spatial gradients (indicative of areal transitions) across species. Nevertheless, our candidate chimpanzee PFC boundary between premotor and prefrontal cortex warrants further analysis using modern architectonic and/or imaging methods.

Besides the architectonic, functional, and morphological criteria invoked in our study, other types of information have been proposed for delineating the PFC in various mammalian species. These include the distribution of dopaminergic projections and a prominent level of projections from the MD nucleus of the thalamus (46–48). Neither of these metrics, however, has been shown to be adequately specific to provide strong diagnostic criteria for delineating the PFC (32, 40): Dopaminergic projections are prominent throughout the primate brain and are not demonstrably overrepresented in granular frontal cortex (49, 50) compared with more posterior neocortex. Similarly, MD thalamic projections, while particularly prevalent in granular frontal cortex and thus a meaningful guide, are also present across the precentral motor region as well as more posterior regions (51).

Human PFC Volume Is Disproportionately Large. We used a surface-based approach (1, 2, 4) derived from structural MRI to generate our analysis of cortical volumes. Our sample size includes 60 humans, 29 chimpanzees, and 19 macaques, thereby enabling estimates of variability in each population. We found the proportion of PFC cortical gray matter volume in humans to be up to 1.9-fold greater than in macaques and up to 1.2-fold greater than in chimpanzees. The differences in the proportion of PFC subcortical white matter volume are even more pronounced, with humans exhibiting a 2.4-fold greater proportion than in macaques and a 1.7-fold greater proportion than in chimpanzees. Thus, consistent with several previous studies (2, 5, 6, 12, 23, 26, 27), our results strongly support the hypothesis that the proportion of cortical gray and white matter volumes attributed to frontal association cortex is larger in humans than in nonhuman primates. Furthermore, the absolute size of the conservatively delineated human PFC is 4.5-fold larger than in the chimpanzee, which is especially striking considering the more modest difference in the size of the primary visual cortex (1.9-fold larger in humans). Coupled with the evidence that humans have substantially more PFC white matter volume (23, 27), this points to an impressively greater amount of neural machinery associated with the PFC in humans compared with nonhuman primates.

Scaling relative to total cortical volume, however, is impacted by the similarity in scaling between the PFC and other cortical association areas. Therefore, scaling of PFC volume based on that of primary sensory and motor areas can shed light on allometric differentiation of different cortical regions (12, 23). Our results indicate a hypometric scaling of V1 with respect to cortical volume relative to the hypermetric scaling of PFC (Fig. 4*A*) and a prominently hypermetric scaling of PFC with respect to V1 (Fig. 4*B*). The hypometric scaling of V1 is likely related to the high visual acuity and importance of vision in all three species, resulting in only modest species differences in the size of V1. For area 4, the lack of an allometric scaling relationship prevented an

analogous comparison of slopes. However, it is visually apparent that chimpanzee and human area 4 scale similarly to area V1. The relatively small size of macaque motor cortex is potentially related to its small body size and muscle mass.

Although other studies have argued for a more general scaling up of the human brain compared with nonhuman primates (17, 19), we do not view the idea of a predictive positive allometric scaling as mutually exclusive with a preferential expansion of PFC or association cortex in general. For example, Semendeferi et al. (19) reported that the proportion of the cortical mantle occupied by cortex anterior to the precentral gyrus does not differ significantly between humans and great apes. However, Passingham and Smaers (12), analyzing the size of various cortical regions relative to primary sensory and motor areas, found that the human PFC deviates from the allometric relationship between the PFC and area V1 determined from nonhuman primate species and thus showed disproportionate enlargement (figure 1 and table 1 in ref. 12). Our analyses corroborate those from Passingham and Smaers by revealing a larger ratio of PFC gray matter volume to primary visual cortex in humans compared with nonhuman primates (Fig. 4*B*). However, the slopes reported for the regressions in our study are limited by the inclusion of only three species. Therefore, we emphasize how the regression slopes differ when comparing different regions of cortex: When using total cortical gray matter as a reference, conservative PFC exhibits positive allometry compared with non-PFC and particularly with area V1. Furthermore, the non-PFC delineation still contains highly expanded regions of association cortex in the parietal and temporal lobes, thus biasing its scaling toward isometry and making the findings related to non-PFC cortical volume reported here likely to be conservative.

Defining PFC as anterior to the genu of corpus callosum, Gabi et al. (17) used an isotropic fractionator approach (52) to count neurons and nonneuronal cells as well as gray matter and white matter volumes as measured in 2-mm coronal tissue slabs through one hemisphere in a single brain from each of eight primate species. For humans vs. the average of two macaque species, they reported 10% vs. 7.6% of cortical gray matter, 5.5% vs. 4.5% of white matter, and 8% vs. 7.35% of total cortical neurons belonging to genu-based PFC (table S1 in ref. 17). Thus, for these two species, their results suggest a slightly positive allometric relationship for PFC cortical gray matter and a nearly isometric relationship for neuronal numbers. In the present study, we found a greater species disparity for both genu-based (15% vs. 10%) and parcellation-based (21% vs. 13%) delineations. Our finding that the genu-based approximation underestimates PFC volume (to somewhat different degrees in humans, chimpanzees, and macaques) (Fig. 4) is consistent with the prediction of Schoenemann et al. (26), as noted by others (12, 23, 53).

Along with their allometric analyses, Gabi et al. reported that human neuronal density increases anteriorly to posteriorly, with lowest density at the frontal pole, whereas macaques exhibit a double gradient of high neuronal densities near both the frontal and occipital poles. A complementary perspective comes from cellular neuroanatomical analyses by Elston et al. (54–57), revealing that pyramidal neurons in nonhuman primate granular PFC (and in other regions of association cortex such as lateral temporal cortex) exhibit more complex dendritic structure (size of basal dendritic arbors, branching structure, and spine density) compared with the less elaborate dendritic structure found in evolutionarily conserved regions such as sensorimotor and early visual cortex (56). In this context, neuron number or density is not a simple surrogate for the information-processing complexity handled by any given brain region. Thus, the differential increase in PFC volume documented in the present study likely in part reflects increased synaptic machinery and not simply an increased number of PFC neurons in the human lineage.

White Matter Underlying Human PFC Is Particularly Large Compared with Nonhuman Primates. We found that human PFC white matter volume (as a percentage of total white matter) is 2.4-fold greater than in the macaque and 1.7-fold greater than in the chimpanzee (Fig. 4*C* and Table 2), corroborating earlier reports (23, 27). It is intriguing to speculate on the neuroanatomical basis of these striking species differences. Given the aforementioned evidence (17) that PFC neuronal density is relatively low in humans vs. nonhuman primates, the density of output axons from human PFC projection neurons (i.e., pyramidal cells) is presumably lower as well. A disproportionately large white matter volume underlying human PFC might instead reflect (*i*) an increased density of afferent projections from distant (non-PFC) regions contributing to an increased axonal density within human PFC gray matter; (*ii*) a disproportionately high percentage of human PFC output axons that traverse the underlying white matter but nonetheless terminate within other PFC targets; (*iii*) a disproportionately large average axonal diameter in human PFC white matter; and/or (*iv*) a disproportionately high degree of axonal branching within human PFC white matter. Disentangling these and other possibilities is unlikely to be easy but might become feasible with further advances in neuroanatomical methods.

Improving the Granularity of Interspecies Comparisons. Our analysis has focused on measurements of the PFC in its entirety, even though it is very heterogeneous in its internal organization, connectivity, and function. Previous comparisons between macaque and human that used interspecies surface-based registration (4, 5) provided evidence that relative expansion in the human lineage is highly nonuniform within the PFC as well as in other higher-cognitive regions (e.g., lateral parietal and temporal cortex) relative to early sensory and motor regions. However, such "evolutionary expansion" maps should be interpreted with caution, given that (*i*) some of the candidate homologs are plausible but not firmly established and (*ii*) the surface-based registration algorithm used to constrain the interspecies mapping tolerated local nonuniformities that are not well-grounded neurobiologically. Recent algorithmic improvements in surface-based registration such as the Multimodal Surface Matching (MSM) method (58, 59) should help address the latter problem when adapted to interspecies registration constraints. The former problem (identifying candidate homologs) should benefit from recent advances in parcellating human cortex (34) and in characterizing its network organization (especially resting-state networks), combined with recent and prospective advances in parcellating macaque cortex and characterizing its network organization.

Methods

Data Collection. We used publicly available healthy young adult human structural T1w and T2w scans acquired at 0.7-mm isotropic resolution as part of the HCP, using the HCP's standard protocol (60). Although we were able to balance by sex in choice of human subjects, this was not feasible for nonhuman primates due to data availability. From a larger HCP subject set, 60 unrelated subjects (30 male and 30 female) were selected for analysis from the S500 HCP data release. Human data were acquired, processed, and publicly released by the Human Connectome Project (HCP). The HCP obtained informed consent from all participants and was approved to conduct human studies by the Washington University in St. Louis Institutional Review Board (#201105040 date: June 2, 2011). For the macaque and chimpanzee structural T1w and T2w scans we used data previously acquired at the Yerkes National Primate Research Center at Emory University. A group of 19 adult macaques (1 male and 18 female) was scanned at 0.5-mm isotropic resolution. A group of 29 adult chimpanzees (all female) was scanned at 0.8-mm isotropic resolution. For the macaque and chimpanzee datasets, localized signal dropout was observed in anterior insular and orbitofrontal cortex. Nonhuman primate data were acquired through separate studies covered by animal research protocols approved by the relevant institutional committees.

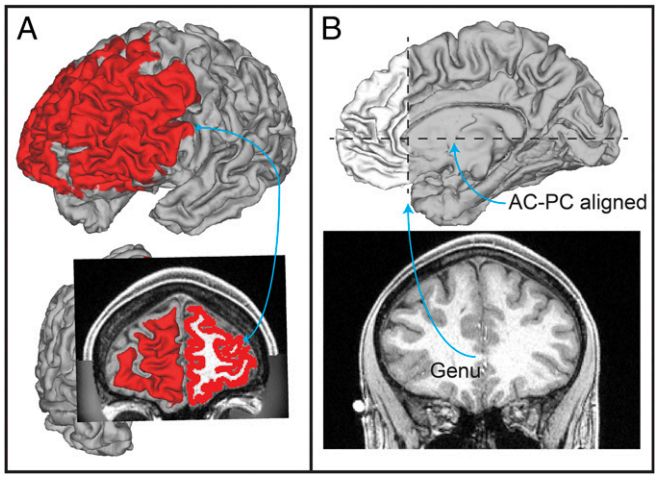

Fig. 5. Mapping of surface-based ROI to cortical gray matter ribbon volume. (*A*) Illustration of human cortical surface ROI mapped to underlying gray matter ribbon volume. (*B*) Illustration of human genu-based ROI volume anterior to a coronal slice at the genu of the corpus callosum when the image is AC–PC aligned.

Image Preprocessing. For each human subject, T1w and T2w scans were initially processed using the minimal preprocessing pipelines developed for the HCP (60) to maximize alignment across imaging modalities and minimize distortions and blurring of the data. Field maps were available, and readout distortion was corrected in humans. Intersubject registration to a group-average atlas surface was performed using a two-stage process based on the MSM algorithm (58), where an initial gentle stage is driven by cortical folding patterns and a more aggressive second stage utilizes cortical areal features of myelin, resting-state network maps, and visuotopic maps (34).

A version of the HCP pipelines adapted for nonhuman primates (HCP-NHP pipelines) (39) was used to process macaque and chimpanzee T1w and T2w structural scans. Initially, the PreFreeSurfer pipeline aligns T1w and T2w volumes to native anterior commissure–posterior commissure (AC–PC) space and performs brain extraction, cross-modal registration, bias field correction, and nonlinear volume registration to atlas space using the FMRIB Software Library (FSL; University of Oxford) (61).

A nonhuman primate-specific pipeline, FreeSurferNHP, differs from the HCP FreeSurfer pipeline in the following ways: (*i*) using nonhuman primate volume templates and adjusting the brain size parameter to 80 mm for the macaque and 120 mm for the chimpanzee and (*ii*) converting the data into a "fake" 1-mm × 1-mm × 1-mm space to conform to FreeSurfer requirements without interpolation (62). This last modification allows the full resolution of the nonhuman primate data to be used for surface generation. Species-specific volume and surface templates were used for registration before transformation back into the 0.5-mm input space. Cortical thickness is then computed, modifying the maximum cortical thickness parameter (from a default value of 5 mm) in the FreeSurfer *mris_make_surfaces* command to conform to scan resolution as 5/resolution mm to ensure that the fake 1-mm space does not set too low a cap on the cortical thickness (0.5 mm data faked to 1 mm would make a 5-mm cortical thickness limit into a 2.5-mm cortical thickness limit if not adjusted).

The PostFreeSurfer pipeline uses MSM-Sulc surface registration, a version of MSM where alignment is driven by cortical shape [FreeSurfer's "sulc" (sulcal) measure]. The pipeline produces a high-resolution 164-k surface mesh (~164,000 vertices per hemisphere), as well as two lower-resolution meshes (32 k/10 k for macaque and 32 k/20 k for chimpanzee). In addition to surface reconstruction, myelin maps (average maps of myelin content across the cortical layers) are created based on the T1w/T2w ratio (6, 45, 60). However, the cortical thickness and myelin maps are likely biased in regions of localized signal dropout (anterior insular and orbitofrontal cortex) because of an imperfect cortical segmentation.

Group-Average Atlases and Cortical Parcellations. Individual subject registration to a group-average atlas enables accurate comparisons across subjects. The HCP Multimodal Parcellation [HCP_MMP1.0 (34)] provided both an atlas space for registration of individual human subjects and a cortical areal classifier for creating individual-subject parcellations. This classifier identified the 180 cortical areas per hemisphere if the fingerprint of each area was detected but allowed the identification of fewer areas. These areas vary in size and shape relative to the original areas defined using group-average data. Additionally, a more accurate medial wall was created to restrict analyses to neocortex and transitional cortex (but excluding the hippocampal formation medial to the presubiculum).

The Yerkes19 macaque surface-based atlas (39) was created using the 19 previously described adult macaque subjects. The HCP-NHP pipelines were used to extract cortical surfaces and subcortical volumes from structural MRI scans. Interhemispheric alignment was driven by 45 geographically corresponding landmark contours per hemisphere, analogous to the landmark-based alignment performed for the F99 macaque surface-based atlas (2). The Ferry et al. (36), Lewis and Van Essen (37), and Paxinos et al. (38) histological parcellations were mapped to the Yerkes19 atlas from the F99 atlas (36, 38, 63) using the MSM algorithm driven by a combination of cortical folding (mean curvature) and revised medial walls (excluding hippocampal cortex medial to the presubiculum) for both atlases. Mean curvature was used as a registration constraint because an accurate FreeSurfer-based sulc map was not available for the F99 atlas surface, which had been generated using the SureFit segmentation method (3) that does not produce the white matter surface required to create a sulc map.

The Yerkes29 chimpanzee surface-based atlas was created in a similar fashion, using the 29 previously described adult chimpanzee subjects. The Bailey et al. cytoarchitectural atlas (42) was used to systematically map cortical areas from published coronal volume slices to the Yerkes29 atlas. Images of histological slice drawings (intermediate between coronal and axial planes) taken from the Bailey et al. atlas were visually matched to corresponding slices in an individual chimpanzee MRI structural scan, using an individual chimpanzee (Edwina) whose frontal convolutions were like those in the atlas, based on visual inspection. These coronal areal designations were then projected to the cortical group average surface based on Bailey et al.'s cortical surface figures and our group-average maps of myelin and sulcal depth.

Delineations approximating PFC based on the genu of the corpus callosum were created by identifying the coronal slice precisely anterior to the genu when individuals were aligned so that the axial slice was parallel to the AC–PC line. All gray and white matter anterior to this coronal slice was considered part of this genu-defined region.

Assigning Prefrontal Cortical Areas. Individual cortical areas were identified as belonging to PFC based on published criteria and delineations (28–30, 42, 64). For each cortical area located in the frontal lobe, primary qualities tabulated included previously published areal classification as PFC and the histological description of areal cortical layer IV (granular, dysgranular, lightly granular, or agranular). Cytoarchitectonically granular/dysgranular areas were included in the delineation of conservative PFC, and agranular areas associated with cognitive-related function were additionally included in the liberal PFC delineation. Additional information about the studies used to define PFC delineations is provided in *Supporting Information* and Tables S2 and S3.

Delineating Areas V1 and 4. To identify area V1, we used the HCP_MMP1.0 (34) for delineation of V1 in the human, myelin maps plus the Lewis and Van Essen parcellation (37) for delineation in the macaque, and myelin maps plus the Bailey et al. cytoarchitectural atlas (42) for delineation in the chimpanzee. Area 4 was identified in humans using the HCP_MMP1.0 parcellation; for chimpanzees and macaques, delineations were based mainly on group-average myelin and cortical thickness maps and their gradients, while also striving for consistency with published atlases (38, 65) (see areal delineations in Fig. 2 and Fig. S4).

Calculation of Cortical Gray Matter and White Matter Volumes. Total cortical volumes were determined by isolating the cortical gray matter ribbon (as defined by the space between white and pial surfaces) and the underlying white matter [as defined by FreeSurfer segmentation (62, 66)] in the native subject space. Total cortical surface areas and mean cortical thicknesses were computed for each subject using the native midthickness surface mesh and excluding the medial wall, using a revised medial wall demarcation for the macaque (i.e., excluding hippocampal cortex and other minor adjustments) rather than a published version (39). For each conservative and liberal parcellation-based PFC delineation, constituent areas were adjoined to create contiguous PFC surface-based ROIs. In humans, these ROIs were created on each subject's 32-k mesh using each subject's individual HCP_MMP1.0 parcellation and then were mapped to each subject's native space using an existing mapping between the two mesh resolutions. In macaques, these ROIs were created on a 164-k mesh using the composite parcellation defined on the Yerkes19 group-average surface and subsequently were registered to each subject's native surface mesh. Similarly, the chimpanzee ROIs were created

on the Yerkes29 164-k surface mesh and were mapped to native subject meshes. Genu-based ROIs were created by including all surface vertices rostral to a coronal slice of the AC–PC aligned volume at the genu of the corpus callosum, an approximation of PFC used in previous studies (17, 26). Volume measurements were determined by summing the volumes of individual polyhedral wedges within each ROI, where each wedge is defined by a triangle in the white surface and the corresponding triangle in the pial surface. This process was performed on each individual subject (human, $n = 60$; macaque, $n = 19$; chimpanzee, $n = 29$), and the mean and SD of all subjects were reported for each case (Table 1). This process is illustrated for an exemplar human in Fig. 5.

Data Availability. All data related to this study are freely available via the BALSA database (https://balsa.wustl.edu/) at https://balsa.wustl.edu/study/show/zlVX.

ACKNOWLEDGMENTS. We thank T. Coalson and E. Reid for technical contributions and C. Sherwood for helpful suggestions and critiques during the review and revision process. This work was supported by NIH Grants T32EB014855 (to C.J.D.), F30MH097312 (to M.F.G.), and R01MH60974 (to D.C.V.E.). Human datasets were provided by the Human Connectome Project, Washington University-University of Minnesota Consortium U54MH091657 (principal investigators: D.C.V.E. and Kamil Ugurbil), funded by the 16 NIH Institutes and Centers that support the NIH Blueprint for Neuroscience Research, and by the McDonnell Center for Systems Neuroscience at Washington University. Macaque and chimpanzee datasets were provided through support from NIH Grant P01AG026423, National Center for Research Resources Grant P51RR165 (superseded by the Office of Research Infrastructure Programs/OD P51OD11132), and National Chimpanzee Brain Resource Grant R24NS092988.

1. Van Essen DC, Glasser MF, Dierker DL, Harwell J, Coalson T (2012) Parcellations and hemispheric asymmetries of human cerebral cortex analyzed on surface-based atlases. *Cereb Cortex* 22:2241–2262.
2. Van Essen DC, Glasser MF, Dierker DL, Harwell J (2012) Cortical parcellations of the macaque monkey analyzed on surface-based atlases. *Cereb Cortex* 22:2227–2240.
3. Van Essen DC (2004) Surface-based approaches to spatial localization and registration in primate cerebral cortex. *Neuroimage* 23(Suppl 1):S97–S107.
4. Van Essen DC, Dierker DL (2007) Surface-based and probabilistic atlases of primate cerebral cortex. *Neuron* 56:209–225.
5. Orban GA, Van Essen D, Vanduffel W (2004) Comparative mapping of higher visual areas in monkeys and humans. *Trends Cogn Sci* 8:315–324.
6. Glasser MF, Goyal MS, Preuss TM, Raichle ME, Van Essen DC (2014) Trends and properties of human cerebral cortex: Correlations with cortical myelin content. *Neuroimage* 93:165–175.
7. Rolls ET, Grabenhorst F (2008) The orbitofrontal cortex and beyond: From affect to decision-making. *Prog Neurobiol* 86:216–244.
8. Murray EA, O'Doherty JP, Schoenbaum G (2007) What we know and do not know about the functions of the orbitofrontal cortex after 20 years of cross-species studies. *J Neurosci* 27:8166–8169.
9. Bechara A, Damasio H, Damasio AR (2000) Emotion, decision making and the orbitofrontal cortex. *Cereb Cortex* 10:295–307.
10. Preuss TM (2011) The human brain: Rewired and running hot. *Ann N Y Acad Sci* 1225(Suppl 1):E182–E191.
11. Preuss TM (2017) The human brain: Evolution and distinctive features. *On Human Nature: Biology, Psychology, Ethics, Politics, and Religion*, eds Tibayrenc M, Ayala FJ (Elsevier, London), 1st Ed, pp 125–149.
12. Passingham RE, Smaers JB (2014) Is the prefrontal cortex especially enlarged in the human brain allometric relations and remapping factors. *Brain Behav Evol* 84: 156–166, and erratum (2015) 85:76.
13. Mars RB, Passingham RE, Neubert F-X, Verhagen L, Sallet J (2017) Evolutionary specializations of human association cortex. *Evolution of Nervous Systems*, eds Kaas JH, Preuss TM (Elsevier, New York), 2nd Ed, pp 185–205.
14. Blinkov SM, Glezer II (1968) *The Human Brain in Figures and Tables* (Basic Books, New York).
15. Brodmann K (1912) Neue Ergebnisse über die vergleichende histologische Lokalisation der Grosshirnrinde mit besonderer Berücksichtigung des Stirnhirns. *Anat Anz* 41(Suppl):157–216.
16. Geschwind N (1965) Disconnexion syndromes in animals and man. I. *Brain* 88:237–294.
17. Gabi M, et al. (2016) No relative expansion of the number of prefrontal neurons in primate and human evolution. *Proc Natl Acad Sci USA* 113:9617–9622.
18. Barton RA, Venditti C (2013) Human frontal lobes are not relatively large. *Proc Natl Acad Sci USA* 110:9001–9006.
19. Semendeferi K, Lu A, Schenker N, Damasio H (2002) Humans and great apes share a large frontal cortex. *Nat Neurosci* 5:272–276.
20. Sherwood CC, Smaers JB (2013) What's the fuss over human frontal lobe evolution? *Trends Cogn Sci* 17:432–433.
21. Schoenemann PT (1997) An MRI study of the relationship between human neuroanatomy and behavioral ability. Available at www.indiana.edu/~brainevo/publications/dissertation/Dissertation_title.htm. Accessed December 1, 2017.
22. Bush EC, Allman JM (2004) The scaling of frontal cortex in primates and carnivores. *Proc Natl Acad Sci USA* 101:3962–3966.
23. Smaers JB, Gómez-Robles A, Parks AN, Sherwood CC (2017) Exceptional evolutionary expansion of prefrontal cortex in great apes and humans. *Curr Biol* 27:714–720.
24. Semendeferi K, Damasio H (2000) The brain and its main anatomical subdivisions in living hominoids using magnetic resonance imaging. *J Hum Evol* 38:317–332.
25. Chaplin TA, Yu H-H, Soares JGM, Gattass R, Rosa MGP (2013) A conserved pattern of differential expansion of cortical areas in simian primates. *J Neurosci* 33:15120–15125.
26. Schoenemann PT, Sheehan MJ, Glotzer LD (2005) Prefrontal white matter volume is disproportionately larger in humans than in other primates. *Nat Neurosci* 8:242–252.
27. Smaers JB, et al. (2011) Primate prefrontal cortex evolution: Human brains are the extreme of a lateralized ape trend. *Brain Behav Evol* 77:67–78.
28. Ongür D, Ferry AT, Price JL (2003) Architectonic subdivision of the human orbital and medial prefrontal cortex. *J Comp Neurol* 460:425–449.
29. Carmichael ST, Price JL (1994) Architectonic subdivision of the orbital and medial prefrontal cortex in the macaque monkey. *J Comp Neurol* 346:366–402.
30. Petrides M, Pandya DN (2002) Comparative cytoarchitectonic analysis of the human and the macaque ventrolateral prefrontal cortex and corticocortical connection patterns in the monkey. *Eur J Neurosci* 16:291–310.
31. Petrides M, Pandya DN (1999) Dorsolateral prefrontal cortex: Comparative cytoarchitectonic analysis in the human and the macaque brain and corticocortical connection patterns. *Eur J Neurosci* 11:1011–1036.
32. Preuss TM (1995) Do rats have prefrontal cortex? The rose-woolsey-akert program reconsidered. *J Cogn Neurosci* 7:1–24.
33. Geyer S (2004) The microstructural border between the motor and the cognitive domain in the human cerebral cortex. *Adv Anat Embryol Cell Biol* 174: I–VIII, 1–89.
34. Glasser MF, et al. (2016) A multi-modal parcellation of human cerebral cortex. *Nature* 536:171–178.
35. Walker AE (1940) A cytoarchitectural study of the prefrontal area of the macaque monkey. *J Comp Neurol* 73:59–86.
36. Ferry AT, Ongür D, An X, Price JL (2000) Prefrontal cortical projections to the striatum in macaque monkeys: Evidence for an organization related to prefrontal networks. *J Comp Neurol* 425:447–470.
37. Lewis JW, Van Essen DC (2000) Mapping of architectonic subdivisions in the macaque monkey, with emphasis on parieto-occipital cortex. *J Comp Neurol* 428:79–111.
38. Paxinos G, Huang X-F, Toga A (2000) *The Rhesus Monkey Brain in Stereotaxic Coordinates* (Academic, San Diego).
39. Donahue CJ, et al. (2016) Using diffusion tractography to predict cortical connection strength and distance: A quantitative comparison with tracers in the monkey. *J Neurosci* 36:6758–6770.
40. Passingham RE, Wise SP (2012) *The Neurobiology of the Prefrontal Cortex: Anatomy, Evolution, and the Origin of Insight* (Oxford Univ Press, Oxford).
41. Wise SP (2008) Forward frontal fields: Phylogeny and fundamental function. *Trends Neurosci* 31:599–608.
42. Bailey P, Bonin GV, McCulloch WS (1950) *The Isocortex of the Chimpanzee* (Univ of Illinois Press, Urbana, IL).
43. Murray EA, Wise SP, Graham KS (2016) *The Evolution of Memory Systems* (Oxford Univ Press, Oxford).
44. Schall JD, Morel A, King DJ, Bullier J (1995) Topography of visual cortex connections with frontal eye field in macaque: Convergence and segregation of processing streams. *J Neurosci* 15:4464–4487.
45. Glasser MF, Van Essen DC (2011) Mapping human cortical areas in vivo based on myelin content as revealed by T1- and T2-weighted MRI. *J Neurosci* 31: 11597–11616.
46. Rose JE, Woolsey CN (1948) The orbitofrontal cortex and its connections with the mediodorsal nucleus in rabbit, sheep and cat. *Res Publ Assoc Res Nerv Ment Dis* 27: 210–232.
47. Akert K (1964) Comparative anatomy of frontal cortex and thalamofrontal connections. *The Frontal Granular Cortex and Behavior*, eds Warren JM, Akert K (McGraw-Hill, New York), pp 372–396.
48. Uylings HBM, Groenewegen HJ, Kolb B (2003) Do rats have a prefrontal cortex? *Behav Brain Res* 146:3–17.
49. Gaspar P, Stepniewska I, Kaas JH (1992) Topography and collateralization of the dopaminergic projections to motor and lateral prefrontal cortex in owl monkeys. *J Comp Neurol* 325:1–21.
50. Williams SM, Goldman-Rakic PS (1998) Widespread origin of the primate mesofrontal dopamine system. *Cereb Cortex* 8:321–345.
51. Matelli M, Luppino G (1996) Thalamic input to mesial and superior area 6 in the macaque monkey. *J Comp Neurol* 372:59–87.
52. Herculano-Houzel S, Lent R (2005) Isotropic fractionator: A simple, rapid method for the quantification of total cell and neuron numbers in the brain. *J Neurosci* 25: 2518–2521.
53. Sherwood CC, Holloway RL, Semendeferi K, Hof PR (2005) Is prefrontal white matter enlargement a human evolutionary specialization? *Nat Neurosci* 8:537–538, author reply 538.
54. Elston GN, Benavides-Piccione R, Elston A, Manger PR, Defelipe J (2011) Pyramidal cells in prefrontal cortex of primates: Marked differences in neuronal structure among species. *Front Neuroanat* 5:2.
55. Elston GN, Benavides-Piccione R, Elston A, Manger P, DeFelipe J (2005) Pyramidal cell specialization in the occipitotemporal cortex of the vervet monkey. *Neuroreport* 16: 967–970.
56. Elston GN, Rockland KS (2002) The pyramidal cell of the sensorimotor cortex of the macaque monkey: Phenotypic variation. *Cereb Cortex* 12:1071–1078.
57. Elston GN (2000) Pyramidal cells of the frontal lobe: All the more spinous to think with. *J Neurosci* 20:RC95.

58. Robinson EC, et al. (2014) MSM: A new flexible framework for Multimodal Surface Matching. *Neuroimage* 100:414–426.
59. Robinson EC, et al. (2018) Multimodal surface matching with higher-order smoothness constraints. *Neuroimage* 167:453–465.
60. Glasser MF, et al.; WU-Minn HCP Consortium (2013) The minimal preprocessing pipelines for the Human Connectome Project. *Neuroimage* 80:105–124.
61. Smith SM, et al. (2004) Advances in functional and structural MR image analysis and implementation as FSL. *Neuroimage* 23(Suppl 1):S208–S219.
62. Fischl B (2012) FreeSurfer. *Neuroimage* 62:774–781.
63. Lewis JW, Van Essen DC (2000) Corticocortical connections of visual, sensorimotor, and multimodal processing areas in the parietal lobe of the macaque monkey. *J Comp Neurol* 428:112–137.
64. Frey S, et al. (2011) An MRI based average macaque monkey stereotaxic atlas and space (MNI monkey space). *Neuroimage* 55:1435–1442.
65. Saleem KS, Logothetis NK (2012) *A Combined MRI and Histology Atlas of the Rhesus Monkey Brain in Stereotaxic Coordinates* (Academic, New York).
66. Fischl B, et al. (2002) Whole brain segmentation: Automated labeling of neuroanatomical structures in the human brain. *Neuron* 33:341–355.